

Reactive Power Cost From PV Inverters Considering Inverter Lifetime Assessment

Oktoviano Gandhi , Student Member, IEEE, Carlos D. Rodríguez-Gallegos , Student Member, IEEE,

Naga Brahmendra Yadav Gorla, Student Member, IEEE, Monika Bieri, Thomas Reindl,

and Dipti Srinivasan, Senior Member, IEEE

Abstract—Photovoltaic (PV) system inverters have been frequently utilized for reactive power support in the literature. Although the benefits of PV reactive power for the grid have been quantified, the costs incurred by the PV owner have largely been ignored. This paper combines the findings from power electronics research and power system economics to formulate the cost of reactive power from PV inverters, considering the inverter degradation due to the reactive power provision. One-year simulations with real weather and load data for the case of Singapore for different levels of PV penetration have been conducted. Subsequently, the benefits of local reactive power provision to the system and its effect on the lifetime of PV inverters were analyzed. It was found that the cost of inverter lifetime reduction is a significant part of the reactive power cost (more than 50% at lower PV penetration), but decreases at higher PV penetration when the reactive power support is distributed over more PV systems. Through comprehensive analysis, the feasible range for monetary incentives for PV reactive power support has been identified. The results from this paper can, therefore, be used as a foundation for future research, formulating regulations, and for market analysis.

Index Terms—Inverters, photovoltaic systems, power system economics, reactive power.

I. INTRODUCTION

R EACTIVE power support is important in keeping voltage magnitudes of a power system within a specified range. To reduce the amount of reactive power transported in the network,

Manuscript received December 24, 2017; revised May 2, 2018; accepted May 31, 2018. Date of publication June 12, 2018; date of current version March 21, 2019. Paper no. TSTE-01172-2017. (Corresponding author: Oktoviano Gandhi.)

O. Gandhi is with the Graduate School of Integrative Sciences and Engineering, National University of Singapore, Singapore 117456, and also with the Solar Energy Research Institute of Singapore, National University of Singapore, Singapore 117574 (e-mail: oktoviano.gandhi@u.nus.edu).

C. D. Rodríguez-Gallegos is with the Solar Energy Research Institute of Singapore, National University of Singapore, Singapore 117574, and also with the Department of Electrical and Computer Engineering, National University of Singapore, Singapore 117576 (e-mail: carlos.rodriguez@nus.edu.sg).

N. Brahmendra and D. Srinivasan are with the Department of Electrical and Computer Engineering, National University of Singapore, Singapore 117576 (e-mail: naga@u.nus.edu; dipti@nus.edu.sg).

M. Bieri is with the Cleantech Energy Corporation Limited, Singapore 049482 (e-mail: monika.bieri@cleantechsolar.com).

T. Reindl is with the Solar Energy Research Institute of Singapore, National University of Singapore, Singapore 117574 (e-mail: thomas.reindl@nus.edu.sg).

Color versions of one or more of the figures in this paper are available online at <http://ieeexplore.ieee.org>.

Digital Object Identifier 10.1109/TSTE.2018.2846544

and hence the line loading, sources of reactive power need to be distributed throughout the system [1].

Meanwhile, adoption of solar energy has been increasing rapidly in the past decades. Its installations, in the form of photovoltaic systems (PVs), are more geographically distributed compared to conventional generation. The inverter-based PV are able to generate both active and reactive power [2]. In many works, PV has been used to provide local reactive power support in distribution systems and microgrids [3]–[10]. The local reactive power provision has been shown to reduce losses [3]–[6], decrease line loading [8], [9], maintain the systems' voltage within limits [5]–[8], and reduce the cost of running the system [8], [9].

Even though many researchers assume that PV inverters are able to inject reactive power at no cost [3], [6]–[8], there are tradeoffs involved in producing reactive power through the inverter. The first tradeoff is the additional losses in the inverter because of the reactive power usage [5], [11], which either reduces the active power output of the PV or has to be compensated by the grid [4], [11], [12]. However, there is another trade-off in providing reactive power using inverters, which has not been taken into account by power system or optimization researchers, namely the increase in wear and tear of the inverter components.

The increased wear and tear has been analysed by power electronics researchers, and shown to reduce the lifetime of the inverter. The additional losses from reactive power injection cause temperature rise in the inverter components, especially during the time when PV is not generating any active power [13], [14]. Consequently, increase in thermal stress has adverse impacts on the lifetime of inverter components [13], [15]–[18]. Therefore, the detrimental effects of reactive power injection on the PV inverter lifetime can be analysed in depth at the component level. Nevertheless, no work to date has translated the lifetime reduction (LR) due to the injection to a cost borne by the PV owners or the power system operators. However, this is of utmost importance for both the PV owners and power system operators to determine the viability of PV to inject reactive power as ancillary services. The main aim of PV owners is generally to receive as much compensation as possible – subject to satisfying grid requirements – either through the active power generation, or provision of ancillary services. Therefore, PV reactive power provision needs to be accompanied by suitable monetary incentives. With rapid increase of PV penetration, timely investigation is imperative so that appropriate regulations

can be implemented and costly retrofitting of the PV systems or change in the regulations can be avoided [19].

In this work, effects of reactive power injection from PV inverters on the inverter LR have been quantified into an increase in the levelised cost of electricity (LCOE) of the PV system, which is then further translated into reactive power cost. Subsequently, this work expands the existing literature by analysing the costs and benefits of PV reactive power compensation at different penetration levels. The net benefits for the system are also evaluated such that the feasible payment range for the reactive power service can be determined. Although in this work only reactive power injection is being considered, the insights can be adapted for the case of reactive power absorption.

Hence, the contributions of this paper are:

- 1) Translating the reduction in inverter lifetime due to reactive power injection into reactive power cost for PV
- 2) Establishing a relationship between PV reactive power output and the inverter lifetime, which can be incorporated into any cost function and optimization problem
- 3) Identifying the feasible range for monetary incentives for PV owners to provide reactive power compensation

The rest of the work is laid out as follows: Section II describes the modeling of PV and constraints on PV reactive power provision. In Section III, the impact of reactive power injection on the inverter lifetime is analysed and translated into reactive power cost. Section IV describes the method to optimize the reactive power dispatch. The case studies, as well as the inverter and system configurations are presented in Section V. The results of the investigation of the costs and benefits of reactive power provision from PV inverters are then discussed in Section VI, and finally Section VII concludes the work.

II. REACTIVE POWER PROVISION BY PV

The active power generation of PV at any particular time period t depends on the irradiance (G_t) and ambient temperature (T_t^a). Experimentally validated PV module model has been adopted from [20], which gives the values of PV module current (I_t^{PV}) and voltage (V_t^{PV}) at any particular period t , given the weather condition. They are described by the following equations:

$$I_t^{\text{PV,SC}} = I_{\text{ref}}^{\text{PV,SC}} \left[1 + \alpha (T_t^{\text{PV}} - T_{\text{ref}}^{\text{PV}}) \right] \frac{G_t}{G_{\text{ref}}} \quad (1)$$

$$I_t^{\text{PV}} = I_{\text{ref}}^{\text{PV}} \frac{I_t^{\text{PV,SC}}}{I_{\text{ref}}^{\text{PV,SC}}} \quad (2)$$

$$V_t^{\text{PV,OC}} = V_{\text{ref}}^{\text{PV,OC}} \left[1 + \beta (T_t^{\text{PV}} - T_{\text{ref}}^{\text{PV}}) + \gamma \ln \left(\frac{G_t}{G_{\text{ref}}} \right) \right] \quad (3)$$

$$V_t^{\text{PV}} = V_{\text{ref}}^{\text{PV}} + (V_t^{\text{PV,OC}} - V_{\text{ref}}^{\text{PV,OC}}) + R^{\text{PV,s}} (I_{\text{ref}}^{\text{PV}} - I_t^{\text{PV}}) \quad (4)$$

where $I_t^{\text{PV,SC}}$ and $V_t^{\text{PV,OC}}$ represents the short circuit current and the open circuit voltage of the PV module respectively. The subscript ‘ref’ represents a reference value that can be obtained from datasheet of a particular PV module. α , β , and γ are the temperature coefficient of $I_t^{\text{PV,SC}}$, temperature coefficient of $V_t^{\text{PV,OC}}$,

and the irradiance correction factor of $V_t^{\text{PV,OC}}$ respectively. The series resistance, $R^{\text{PV,s}}$, is calculated using the formula in [20].

T_t^{PV} is the temperature of the solar cells and can be calculated using [21]:

$$T_t^{\text{PV}} = T_t^a + \frac{G_t}{800[\text{W/m}^2]} (\text{NOCT}-20[\text{°C}]) \quad (5)$$

where NOCT is the nominal operating cell temperature.

PV systems consist of many modules arranged in series and parallel. The active power output of such system, P_t^{PV} , can be obtained using:

$$P_t^{\text{PV}} = N^{\text{PV,par}} I_t^{\text{PV}} \times N^{\text{PV,ser}} V_t^{\text{PV}} \times PR' - P_t^{\text{PV,invloss}} \quad (6)$$

where $N^{\text{PV,par}}$ is the number of PV strings in parallel, while $N^{\text{PV,ser}}$ is the number of PV connected in series for each string. PR' is defined as the performance ratio of the PV system before taking into account the inverter losses ($P_t^{\text{PV,invloss}}$).

For most of the PV lifetime, P_t^{PV} is less than the rating of the inverter, $S_{\text{max}}^{\text{PV}}$. And the spare capacity of the inverter can be used to generate reactive power. So as not to overload the inverter for prolonged period of time¹ and not to curtail P_t^{PV} , the reactive power injected (or absorbed) by PV, Q_t^{PV} , needs to follow the inequality constraint:

$$|Q_t^{\text{PV}}| \leq \sqrt{(S_{\text{max}}^{\text{PV}})^2 - (P_t^{\text{PV}} + \Delta P_t^{\text{PV}})^2} \quad (7)$$

where ΔP_t^{PV} is the maximum error prediction for active power generation. The uncertainty representation (ΔP_t^{PV}) in (7) is generic and can be replaced depending on the forecasting method, based on the preference of the system operator. Active power curtailment to generate more reactive power than available from (7) has not been taken into account, as it has been shown in [12] that it is not economical to do so as lost opportunity payment has to be reimbursed to the PV owners.

III. REACTIVE POWER COST

A. Power Loss Component

Reactive power injection through PV inverters has been shown to induce additional inverter losses [11] and the resulting reactive power cost has been explicitly formulated [12]:

$$c_t^{\text{QPV, invloss}} Q_t^{\text{PV}} = c_t^{\text{Pgrid}} \times \Delta P_t^{\text{PV,invloss}} \quad (8)$$

where c_t^{Pgrid} is the active power price purchased by the distribution system from the main grid, and $\Delta P_t^{\text{PV,invloss}}$ is the additional power loss in the inverter because of the reactive power injection [12].

B. Inverter Lifetime Reduction Component

On top of the additional losses, reactive power injection also induces higher thermal stress on the inverter components [13], [14]. In particular, capacitors are found to be the components most likely to age faster from thermal and power cycling [15], [16], [22], [23]. Therefore, in this work, the lifetime of the capacitor has been assumed to be the same as the inverter lifetime.

¹The size of time step t considered in this paper is half hour.

$$LCOE = \frac{EPCI + IDC + \sum_{n=1}^N \frac{OM^* + IC^*}{(1+DR)^n} + \frac{IRI_{n=OL,20L,30L,\dots\leq 20}^*}{(1+DR)^n} + \sum_{n=1}^N \frac{LP}{(1+DR)^n} + \frac{RV_{n=20}^*}{(1+DR)^{n=20}}}{\sum_{n=1}^N \frac{(\sum_{t=1}^T P_t^{\text{PV}}) \times (1-SDR)^n}{(1+DR)^n}} \quad (16)$$

*inflation-adjusted

1) Capacitor Degradation: First, the lifetime of the capacitor for a particular operating condition (L_t^{CAP}) can be calculated from the following formula [17]:

$$L_t^{\text{CAP}} = L_0^{\text{CAP}} \left(\frac{V_t^{\text{CAP,DC}}}{V_0^{\text{CAP}}} \right)^{-n} 2^{\frac{T_0^{\text{CAP}} - T_t^{\text{CAP}}}{10}} \quad (9)$$

where L_0^{CAP} , V_0^{CAP} , and T_0^{CAP} are reference lifetime, voltage rating, and temperature rating of the capacitor. n is the voltage stress exponent of the lifetime model. $V_t^{\text{CAP,DC}}$ is the operating voltage of the DC link capacitor, which can be taken to be: $V_t^{\text{CAP,DC}} = \max(V_t^{\text{PV}}, V^{\text{INV,DC}})$ where $V^{\text{INV,DC}}$ is the rated DC voltage of the inverter, that is required to produce the nominal inverter line to line RMS AC output voltage, $V^{\text{INV,AC}}$. Typically, for sinusoidal pulse-width modulation (SPWM) inverters, $V^{\text{INV,DC}} \geq V^{\text{INV,AC}} \times 2\sqrt{2}/\sqrt{3}$ [24].

The temperature of the capacitor, T_t^{CAP} , can be obtained using the following [18]:

$$T_t^{\text{CAP}} = T_t^a + R^{\text{CAP,th}} R^{\text{CAP,s}} \left(I_t^{\text{CAP,ripple}} \right)^2 \quad (10)$$

where $R^{\text{CAP,th}}$ and $R^{\text{CAP,s}}$ are the thermal and series resistances of the capacitor. $I_t^{\text{CAP,ripple}}$ is the ripple current through the capacitor, which can be calculated using [25]:

$$I_t^{\text{CAP,ripple}} = I_t^{\text{CAP,ACrms}} \sqrt{2M_t \left[\frac{\sqrt{3}}{4\pi} + \cos^2 \phi \left(\frac{\sqrt{3}}{\pi} - \frac{9}{16} M_t \right) \right]} \quad (11)$$

where $I_t^{\text{CAP,ACrms}} = \frac{\sqrt{(P_t^{\text{PV}})^2 + (Q_t^{\text{PV}})^2}}{V^{\text{INV,AC}}}$ is the RMS AC current through the capacitor, $\cos\phi$ is the power factor of the inverter, and M_t is the modulation index given by the following [25]:

$$M_t = \frac{2\sqrt{2}V^{\text{INV,AC}}}{\sqrt{3}V_t^{\text{CAP,DC}}} \quad (12)$$

The expected lifetime L_t^{CAP} of the capacitor is different at every t , due to different T_t^{CAP} (Eq. (9)²). Therefore, to get the lifetime in years, the following calculation is carried out:

$$\text{Degradation} = \sum_{t=1}^T \frac{H}{L_t} \quad (13)$$

$$OL = 1/\text{Degradation} \quad (14)$$

where *Degradation* is the total degradation of the capacitor in the first year. In this work, the analyses are done over a year (2016) at half hour resolution, such that $H = \frac{1}{2}$ and $T = 17568$.

² $V_t^{\text{CAP,DC}}$ is always the same in the simulations done, i.e. $V_t^{\text{CAP,DC}} = V^{\text{INV,DC}}$, and therefore can be taken as constant.

OL is the operating lifetime of the inverter, assuming that the weather condition of the subsequent years is the same as the first year.

The lifetime reduction (LR) due to reactive power injection is then:

$$\begin{aligned} LR &= OL^P - OL^Q \\ &= \nu \left(\theta_t - 2^{\lambda_t - \mu Q^2} \right) \end{aligned} \quad (15)$$

where OL^P and OL^Q are the operating lifetime of the capacitor – and hence the inverter – when it is only used for P^{PV} , and for both P^{PV} and Q^{PV} , respectively. The other symbols are defined as:

$$\begin{aligned} \lambda_t &= \frac{1}{10} \left[T_0^{\text{CAP}} - T_t^a - \frac{R^{\text{CAP,th}} R^{\text{CAP,s}} (\zeta + \kappa) (P_t^{\text{PV}})^2}{(V^{\text{INV,AC}})^2} \right] \\ \theta_t &= 2^{\frac{T_0^{\text{CAP}} - T_t^{\text{CAP,P}}}{10}} \quad \mu = \frac{\zeta R^{\text{CAP,th}} R^{\text{CAP,s}}}{10 (V^{\text{INV,AC}})^2} \\ \nu &= L_0^{\text{CAP}} \left(\frac{V_t^{\text{CAP,DC}}}{V_0^{\text{CAP}}} \right)^{-n} \quad \zeta = \frac{2M\sqrt{3}}{4\pi} \\ \kappa &= \frac{\sqrt{3}}{\pi} - \frac{9}{16} M \end{aligned}$$

where $T_t^{\text{CAP,P}}$ is the temperature of the capacitors when the PV inverter is only producing active power.

2) Economic Effect: To integrate LR into a reactive power cost value, the effect of the inverter lifetime reduction needs to be quantified, in this case on the basis of the LCOE of the PV system. LCOE of a PV system can be calculated using (16) shown at the top of this page [26].

As the unit of LCOE is [\$/kWh], the numerator in (16) consists of all the possible costs for a PV system throughout its lifetime (assumed to be 20 years, i.e. $N = 20$), whereas the denominator is the total energy generated by the PV in the 20 years. The equity project cost investment (EPCI), together with the interest during construction (IDC) make up the initial investment cost. The annual operating cost includes the operations and maintenance (OM) and the insurance cost (IC). The inverter replacement investment (IRI) represents the cost to replace inverters every OL th year, where OL is the lifetime of the capacitor in years, calculated using (14). When part of the upfront investment is debt financed (assumed to be 60% here), the loan payments (LP) need to be made every year, including annual interest and amortisation expense. At the end of the 20 years, a residual value (RV) might still be present. The denominator is the sum of the annual energy productions. After the first year, the energy produced is adjusted with the system degradation rate (SDR). Annual values in the numerator and

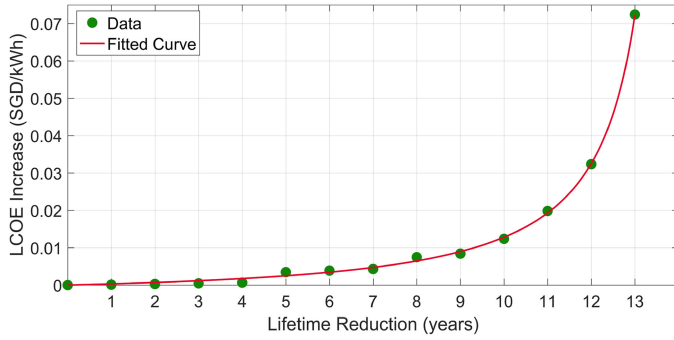


Fig. 1. Relation between the increase in LCOE and lifetime reduction (LR). The data points are fitted with (17). The original inverter lifetime with only active power generation (Case 1) has been set to 14 years, as was found for the system parameters used in this paper. r^2 value is 0.99908.

the denominator are adjusted by the discount rate (DR) for net present value calculations [26], [27].

Because of the inverter lifetime reduction, IRI from equation (16) will increase when the inverter is used for reactive power provision, causing the LCOE of PV to increase. The LCOE increase (LI) for different values of LR is plotted in Fig. 1. It shows that LI can be approximated as:

$$LI[\$/kWh] = \frac{\eta^{LI,A1} LR + \eta^{LI,A0}}{LR^2 + \eta^{LI,B1} LR + \eta^{LI,B0}} \quad (17)$$

where $\eta^{LI,A0}$, $\eta^{LI,A1}$, $\eta^{LI,B0}$, and $\eta^{LI,B1}$ are constants.

To translate the LCOE increase from $[\$/kWh]$ to $[\$]$, (17) is multiplied by P_{Ave}^{PV} , the average active power generated by the PV at each period t over the lifetime of the system, taking into account the reduction in PR in later years. Finally, the reactive power cost due to inverter lifetime reduction, $c_t^{QPV,LR}$, is obtained through the following:

$$c_t^{QPV,LR} Q_t^{PV} = LI[\$] \quad (18)$$

IV. METHODOLOGY

To analyse the importance of the cost of inverter lifetime reduction, a distribution system with reactive-capable PV is considered. The operational cost of running the grid-connected distribution system is given by the following:

$$\begin{aligned} Cost = \sum_{t=1}^T & \left[\underbrace{c_t^{\text{grid}} P_t^{\text{grid}}}_{\text{cost of P from grid}} + \underbrace{c_t^{Q\text{grid}} Q_t^{\text{grid}}}_{\text{cost of Q from grid}} \right. \\ & + \underbrace{\sum_{t=1}^T c_x^{PPV} P_{x,t}^{PV}}_{\text{cost of P from PV}} + \left. \underbrace{\sum_{t=1}^T c_{x,t}^{QPV} Q_{x,t}^{PV}}_{\text{cost of Q from PV}} \right] H \end{aligned} \quad (19)$$

where $c_t^{Q\text{grid}}$ is the reactive power charge from the grid. c_x^{PPV} is the LCOE of the x th PV, as calculated in (16). The reactive power cost is represented by $c_{x,t}^{QPV} = c_{x,t}^{QPV, \text{invloss}} + c_{x,t}^{QPV, \text{LR}}$. P_t^{grid} and Q_t^{grid} are the active and reactive power taken from the grid, whereas $P_{x,t}^{PV}$ and $Q_{x,t}^{PV}$ are the active and reactive power injected by the x th PV. There are X number of PV in the system.

To quantify the costs and benefits of reactive power, the operational costs of the following two cases were compared:

Case 1: The PVs are only generating active power ($Q_{x,t}^{PV}$ is always zero).

Case 2: The PVs are generating reactive power according to the reactive power dispatch strategy based on the analytical method [28], as explained later in this section.

The following terms are defined, and are used in the remainder of this paper:

- Benefits from Q: the monetary benefit of having reactive power injection from PV *without* considering the reactive power cost, $c_{x,t}^{QPV}$. It is mathematically defined as $Cost^{\text{Case 1}} - Cost^{\text{Case 2}} + \sum_{t=1}^T \sum_{x=1}^X c_{x,t}^{QPV} Q_{x,t}^{PV} H$. The benefit does not take into account the reactive power cost.
- Net benefits from Q: the monetary benefit of having reactive power injection from PV, *after* considering both $c_{x,t}^{QPV, \text{invloss}}$ and $c_{x,t}^{QPV, \text{LR}}$. It is mathematically defined as $Cost^{\text{Case 1}} - Cost^{\text{Case 2}}$.

The cost-benefit analysis was conducted with 16 penetration levels (represented by the additions of a new PV into the system, as explained in more detail in Section V-B).

The method for the reactive power dispatch is adopted from [28], where an analytical approach was proposed to optimize reactive power dispatch from inverter-based distributed energy resources – albeit without taking into account the inverter lifetime reduction. The derivation of the approach is elaborated below. The analytical method has been adopted in this work as it has been shown to give as good performance, if not better, compared to conventional optimization methods – namely, particle swarm optimization (PSO), genetic algorithm (GA), and interior point method (IPM) [28]. More importantly, the analytical approach is much faster and more suitable to optimize the one-year dispatch.

The optimal PV reactive power output that will minimize (19) can be found by differentiating (19) w.r.t. $Q_{x,t}^{PV}$ and setting $\partial Cost / \partial Q_{x,t}^{PV} = 0$. To perform the differentiation, first P_t^{grid} , Q_t^{grid} , and $c_{x,t}^{QPV}$ need to be expressed in terms of $P_{x,t}^{PV}$ and $Q_{x,t}^{PV}$. The relations between the grid power and the PV power output are as follows:

$$P_t^{\text{grid}} - \sum_{i=1}^{NN} P_{i,t}^{\text{loss}} - \sum_{i=1}^{NN} P_{i,t}^{\text{load}} + \sum_{x=1}^M P_{x,t}^{PV} = 0 \quad (20)$$

$$Q_t^{\text{grid}} - \sum_{i=1}^{NN} Q_{i,t}^{\text{loss}} - \sum_{i=1}^{NN} Q_{i,t}^{\text{load}} + \sum_{x=1}^M Q_{x,t}^{PV} = 0 \quad (21)$$

where $P_{i,t}^{\text{loss}}$ and $Q_{i,t}^{\text{loss}}$ are the active and reactive power losses on the lines connecting sending node i . $P_{i,t}^{\text{load}}$ and $Q_{i,t}^{\text{load}}$ are the active and reactive power demand at node i respectively. There are NN nodes in the system.

In the analytical approach, the power losses along the distribution lines are approximated by ignoring the second order terms in the losses [29], while maintaining their accuracy. This is done by correlating the approximate total power losses – \tilde{P}^{loss} and \tilde{Q}^{loss} – linearly with the exact loss calculated using backward forward sweep, a power flow algorithm for distribution

systems [28]:

$$P^{\text{loss}} = \eta^{\text{P},0} + \eta^{\text{P},1} \tilde{P}^{\text{loss}}; \quad Q^{\text{loss}} = \eta^{\text{Q},0} + \eta^{\text{Q},1} \tilde{Q}^{\text{loss}} \quad (22)$$

where $\eta^{\text{P},0}$, $\eta^{\text{P},1}$, $\eta^{\text{Q},0}$, and $\eta^{\text{Q},1}$ are the constants obtained from fitting \tilde{P}^{loss} to P^{loss} , and \tilde{Q}^{loss} to Q^{loss} . Meanwhile, \tilde{P}^{loss} and \tilde{Q}^{loss} are calculated using the following:

$$\tilde{P}^{\text{loss}} = \sum_{i=1}^{NN-1} r_i \frac{P_i^2 + Q_i^2}{|\bar{V}_i|^2}, \quad \tilde{Q}^{\text{loss}} = \sum_{i=1}^{NN-1} x_i \frac{P_i^2 + Q_i^2}{|\bar{V}_i|^2} \quad (23)$$

where \bar{V}_i refers to the voltage at the i th node when there is no PV in the system. The index t has been removed to simplify the notations.

For simplicity, we assume that there is only one PV (at node k) in the system. P_t^{grid} and Q_t^{grid} in (20) and (21) can then be simplified to:

$$P^{\text{grid}} = \sum_{i=1}^{NN} P_i^{\text{load}} - P^{\text{PV}} + \eta^{\text{P},0} + \eta^{\text{P},1} \tilde{P}^{\text{loss}} \quad (24)$$

$$Q^{\text{grid}} = \sum_{i=1}^{NN} Q_i^{\text{load}} - Q^{\text{PV}} + \eta^{\text{Q},0} + \eta^{\text{Q},1} \tilde{Q}^{\text{loss}} \quad (25)$$

where \tilde{P}^{loss} and \tilde{Q}^{loss} now take into account the PV active and reactive power injection:

$$\begin{aligned} \tilde{P}^{\text{loss}} &= \sum_{i=1}^{k-1} r_i \frac{(P'_i - P^{\text{PV}})^2 + (Q'_i - Q^{\text{PV}})^2}{|\bar{V}_i|^2} \\ &\quad + \sum_{i=k}^{NN-1} r_i \frac{P'^2_i + Q'^2_i}{|\bar{V}_i|^2} \end{aligned}$$

where P'_i and Q'_i are the original active and reactive power flow of the line connecting the i th node before the PV is added at node k . By expanding the square terms, we get:

$$\begin{aligned} \tilde{P}^{\text{loss}} &= \tilde{P}^{\text{loss,initial}} \\ &\quad + \sum_{i=1}^{k-1} r_i \frac{(P^{\text{PV}})^2 - 2P'_i P^{\text{PV}} + (Q^{\text{PV}})^2 - 2Q'_i Q^{\text{PV}}}{|\bar{V}_i|^2} \end{aligned} \quad (26)$$

where $\tilde{P}^{\text{loss,initial}}$ is the total active power loss in the grid when no PV has been added. The value of $\tilde{P}^{\text{loss,initial}}$ is therefore constant. Likewise, \tilde{Q}^{loss} can also be expanded, with r_i changed to x_i .

Therefore Cost in (19) can be expressed in terms of Q^{PV} . The value of Q^{PV} that minimises the total cost can then be obtained by solving the equation $\frac{\partial \text{Cost}}{\partial Q^{\text{PV}}} = 0$. There are two different expressions for Cost due to the different formula of c_t^{PV} when $P^{\text{PV}} = 0$, and when $P^{\text{PV}} \neq 0$ [12].

Therefore, differentiating Cost w.r.t. Q^{PV} when $P^{\text{PV}} = 0$ yields:

$$Q^{\text{PV}} = \frac{B_k + D_k - E + c^{\text{Qgrid}}/2}{A_k + C_k + F} \quad (27)$$

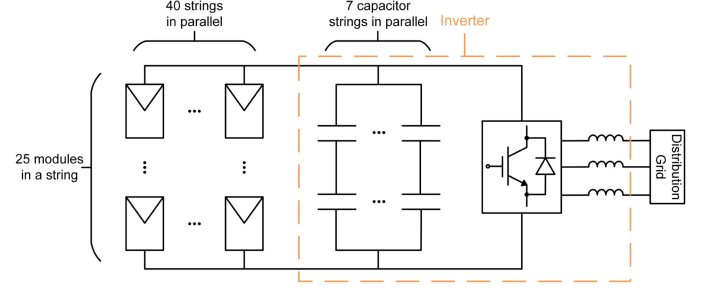


Fig. 2. The configuration of the PV system with a central PV inverter.

where

$$\begin{aligned} A_k &= \sum_{i=1}^{k-1} \frac{r_i}{|\bar{V}_i|^2} c^{\text{Pgrid}} \eta^{\text{P},1}; & C_k &= \sum_{i=1}^{k-1} \frac{x_i}{|\bar{V}_i|^2} c^{\text{Qgrid}} \eta^{\text{Q},1} \\ B_k &= \sum_{i=1}^{k-1} \frac{r_i Q'_i}{|\bar{V}_i|^2} c^{\text{Pgrid}} \eta^{\text{P},1}; & D_k &= \sum_{i=1}^{k-1} \frac{x_i Q'_i}{|\bar{V}_i|^2} c^{\text{Qgrid}} \eta^{\text{Q},1} \\ E &= \frac{c^{\text{Pgrid}} c^{\text{V}}}{2}; & F &= c^{\text{Pgrid}} c^{\text{R}} \end{aligned}$$

When $P^{\text{PV}} \neq 0$, by having $\frac{\partial \text{Cost}}{\partial Q^{\text{PV}}} = 0$, we obtain:

$$\begin{aligned} Q^{\text{PV}} \left(A_k + C_k + F + \frac{E}{\sqrt{(P^{\text{PV}})^2 + (Q^{\text{PV}})^2}} \right) \\ = B_k + D_k + \frac{c^{\text{Qgrid}}}{2} \end{aligned} \quad (28)$$

The full derivation of the analytical approach, its power system constraints, as well as the general details of the approach can be found in [28].

V. IMPLEMENTATION

A. PV-Inverter Configuration

Each PV system is assumed to have a capacity of 300 kWp, composed of 25 Trina 300W modules [30] per string and 40 strings in parallel. The system is connected to a 3-phase 300 kW inverter (Fig. 2). DC link capacitors in the inverter are assumed to be Vishay capacitors 500 PGP-ST [31]. Aluminium electrolytic capacitors have been used as they are the most widely utilized in PV inverters due to their favourable size and cost [15], [16], [25]. Although film capacitors have higher reliability, the adoption of film capacitors is still limited because of higher cost and lower capacitance values for the same volume as electrolytic capacitors [15], [32]. The values for the inverter and capacitor parameters are given in Table I. The value of the thermal resistance of the capacitor, $R^{\text{CAP,th}}$, has been calculated from [18]. The peak inverter efficiency has been assumed to be 98.2% with the inverter efficiency curve from [11].

TABLE I
PARAMETERS

Parameters	Values	Parameters	Values
PV system		Capacitor	
V_{ref}^{PV} [V]	815	C [μF]	15000
$V_{ref}^{PV,OC}$ [V]	997.5	$R^{CAP,s}$ [Ω]	0.009
I_{ref}^{PV} [A]	367.6	$R^{CAP,th}$ [K/W]	1.072
$I_{ref}^{PV,SC}$ [A]	385.6	L_0^{CAP} [h]	3000
Inverter		V_0^{CAP} [V]	400
$V^{INV,DC}$ [V]	800	n	5
$V^{INV,AC}$ [V]	480	No. in series	2
S_{max}^{PV} [kVA]	300	No. in parallel	7

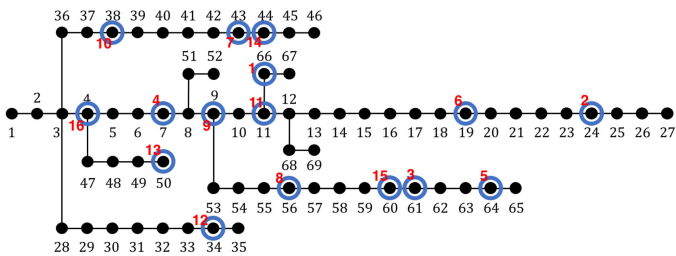


Fig. 3. 69-bus radial distribution system with PV systems. The numbers in red are the order of placement of the PV to analyse the increasing PV penetration.

B. System Data

A 69-bus radial distribution system [33] has been utilised for the test system. The locations and order of adding the PV are shown in Fig. 3.

For the current study, the maximum installed capacity considered is composed of 16 PV systems. This represents 18.0% of the total load demand being provided by PV, also equivalent to 100.6% PV installed capacity compared to peak load (4771 kW). One year Singapore load data from 2016 [34], scaled to the magnitude of the test system's load, has been utilised.

c_t^{grid} is taken from half-hourly wholesale electricity price plus grid charge from Singapore for the year 2016 [35]. The average c_t^{grid} is 8.87 SGD cents per kWh. The average c_t^{grid} when PV is generating power (from 8 a.m. to 6 p.m.) is 9.55 SGD cents per kWh.

LCOE of PV (c_x^{PPV}) is calculated from (16) for the case of Singapore [26]. Assuming inverter lifetime of 14 years – as was found for the system parameters used in this paper – c_x^{PPV} is found to be 10.28 SGD cents per kWh, still higher than the average wholesale electricity price for large electricity consumers.

The solar irradiance and temperature data are also for the year 2016, taken in Singapore at latitude 1.2491° , longitude 103.8414° . They are provided by the Solar Energy Research Institute of Singapore (SERIS).

VI. RESULTS

In this section, first, results comparing the operational costs for the year 2016 (calculated using (19)) of Case 1 and 2 are presented. Subsequently, the effect of reactive power injection

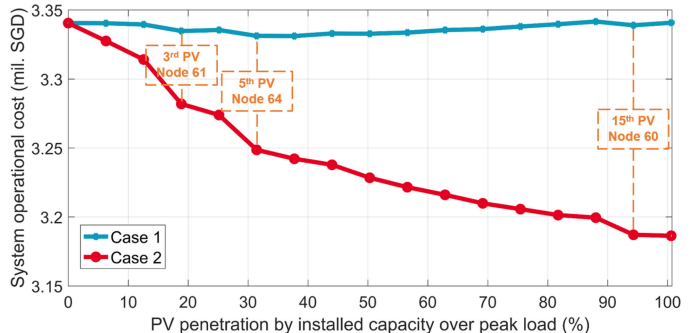


Fig. 4. Operating cost of the system as calculated using (19).

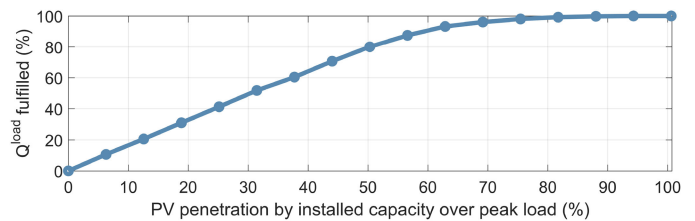


Fig. 5. Percentage of reactive load and losses fulfilled by PV. In this work, the system is not allowed to inject reactive power to the grid.

on the inverter lifetime is analyzed, and the costs and benefits of PV reactive power injection are investigated. Through the results presented in the following subsections, three salient insights can be obtained:

- 1) Reactive power injection from PV is still economically beneficial for the system even after considering the inverter lifetime reduction.
- 2) The reactive power cost due to PV inverter lifetime reduction can be expressed as a cubic or a piecewise quadratic function of the PV reactive power output.
- 3) Inverter lifetime reduction cost is a significant part of the reactive power cost. However, it gradually decreases with increasing PV penetration, when reactive power support is distributed over more PV.

A. Total Operating Costs

When PVs are added into the system, the operational cost of the system decreases even though c_x^{PPV} is higher than the average c_t^{grid} , as can be seen in Fig. 4. When the PVs are only generating active power (Case 1), the cost starts to decrease and reach a minimum when 6 PVs are installed in the system (37.7% penetration by installed capacity). The reduction in cost – despite higher active power cost from PV – comes from the reduced power losses as more PVs are placed in the system. However, the diminishing loss reduction³ cannot compensate for the more costly active power generation from PV and the operational cost increases afterwards.

From Fig. 5, it can be observed that 100% of the reactive load has been fulfilled from 90% penetration level. Nevertheless, as

³This is also partly because the PV system is added randomly, rather than at the most beneficial location for the system. In fact, the power losses increase after the addition of PV at node 38, 34, and 44.

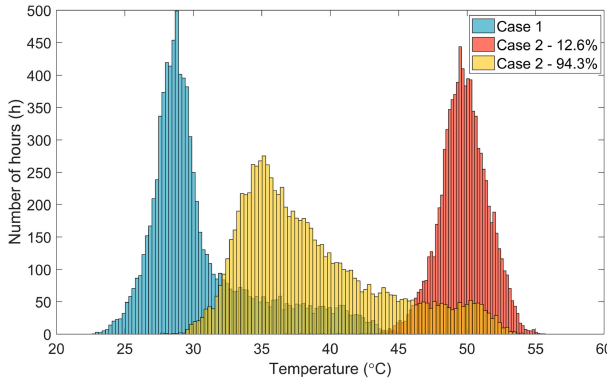


Fig. 6. Temperature profile of the capacitors for PV system at node 66 throughout the year, when the PV is only generating P (blue), generating Q at 12.6% penetration level (red), and at 94.3% penetration level (yellow).

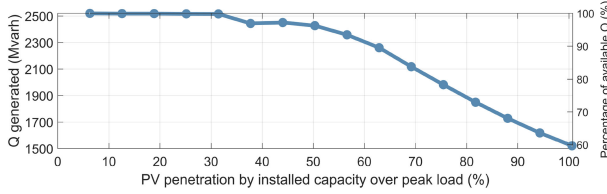


Fig. 7. Average yearly reactive power generated by a PV system at different penetration levels.

observed in Fig. 4, the cost continuously decreases even beyond 90% penetration level. The addition of reactive-capable PV was always economically beneficial for the system regardless of the location. Notably, there was a larger decrease in operational costs when PV is added at strategic locations, namely the third (at node 61), fifth (at node 64), and fifteenth addition (at node 60). Unsurprisingly, all three nodes are located at the same lateral, the most heavily loaded in the system [33].

B. Effects on Inverter Lifetime

When the PV is only generating active power, the inverter is operating at approximately 50% utilisation rate (the sun is shining from 7 a.m. to 7 p.m. throughout the year in our case study), and the capacitors are mostly at ambient temperature, as illustrated by the blue histogram in Fig. 6. The PV penetration does not affect the lifetime of the inverters as $P_{x,t}^{\text{PV}}$ from each PV remains the same regardless of the PV penetration (PV is always operating at maximum power point). In this case, the lifetime of the PV inverter, OL^P , is 14 years.

When PV is also generating reactive power, the inverter components will operate at full utilisation, causing the temperature of the capacitors to increase significantly. It can be seen from Fig. 7 that for PV penetration up to 30%, the PVs are always generating reactive power close to their maximum capacity. This means that the inverters are always operating close to their rated apparent power. However, at 100.6% penetration, the PV systems are only generating approximately 60% of the available reactive power generation (calculated using (7)). That is the reason why the temperatures of the capacitors are on average

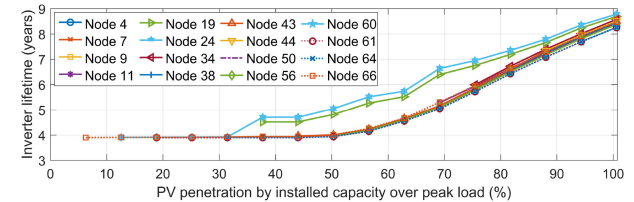


Fig. 8. Lifetime of the PV inverters at different nodes.

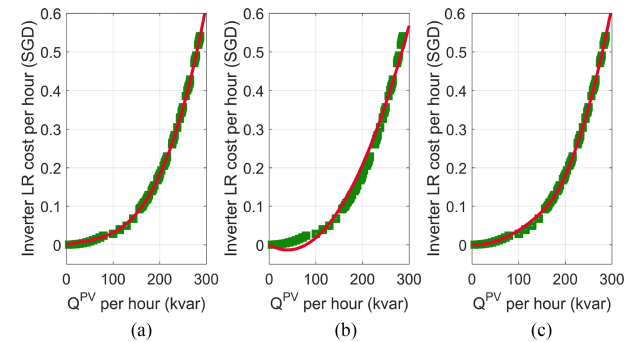


Fig. 9. Relationship between hourly PV reactive power output and hourly inverter LR cost. (a) With cubic fitting. (b) With quadratic fitting. (c) With piecewise quadratic (PQ) fitting. There are two domains for the PQ function shown in (c), namely $Q^{\text{PV}} \leq 150$ kvar and $Q^{\text{PV}} \geq 150$ kvar. At 150 kvar, the two quadratic functions yield approximately the same value. The coefficients of the curves are listed in Table II.

higher when the PV penetration is lower (Fig. 6), as each PV is generating more reactive power at lower penetration levels (Fig. 7). For example, the lifetime of the PV inverter at node 66 is 3.9 and 7.9 years, at 12.6% and 94.3% PV penetration, respectively (Fig. 8).

At the same penetration level, most of the PV inverters have very similar lifetime, except for the PV inverters at node 19 and node 24, which recorded longer lifetimes. These two nodes are located at a lightly loaded lateral and are relatively far away from the other loads (Fig. 3). As such, not as much reactive power is dispatched from them.

By looking at Figs. 7 and 8, a correlation between the reactive power generated and the inverter lifetime can be noted. The existence of such correlation means that (15) and (17) can be simplified into a single variable polynomial equation to be incorporated into an objective function to be optimized. In fact, by plotting the Q generated per hour with the LR cost per hour, the following equation can be obtained (Fig. 9):

$$c_t^{\text{QPV},\text{LR}} Q_t^{\text{PV}} = \eta^{\text{LR},0} + \eta^{\text{LR},1} Q_t^{\text{PV}} + \eta^{\text{LR},2} (Q_t^{\text{PV}})^2 + \eta^{\text{LR},3} (Q_t^{\text{PV}})^3 \quad (29)$$

As shown in Fig. 9 and Table II, the reactive power cost due to inverter LR can be expressed as a cubic function of the reactive power output. Although the quadratic fitting does not fit the simulated data as accurately as the cubic fitting, it was found that a piecewise quadratic (PQ) function fits the data well. The coefficients of the fittings are listed in Table II.

TABLE II
COEFFICIENTS OF THE FITTING

	Cubic	Quadratic	Piecewise Quadratic	
			≤ 150 kvar	≥ 150 kvar
$\eta^{LR,0}$	0	0	0	0.3068
$\eta^{LR,1}$	2.133×10^{-4}	-6.731×10^{-4}	2.768×10^{-5}	3.967×10^{-3}
$\eta^{LR,2}$	-1.986×10^{-6}	8.551×10^{-6}	4.041×10^{-6}	1.667×10^{-5}
$\eta^{LR,3}$	2.726×10^{-8}	0	0	0
r^2	0.99984	0.99159	0.99976	0.99992

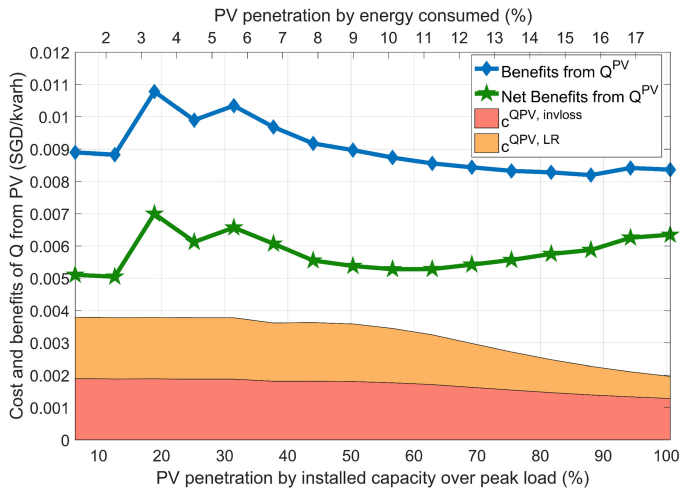


Fig. 10. Average benefits and costs of reactive power provision using PV throughout the year at different penetration levels.

Directly using (15) and (17) to yield the reactive power cost from PV inverter, not only requires involved calculations and knowledge of numerous parameters, but also necessitates the simulation to be run for at least over a year to get an accurate enough lifetime estimation of the inverter⁴. Therefore, through the formulation of (29), $c_t^{QPV, LR}$ can be incorporated into an objective function of an optimization problem with any time horizon.

While the results shown are only for a particular type of inverter and capacitor (to allow for direct comparison), the trend will be similar for other configurations, even if the exact lifetime and cost vary. Such relationship will be crucial for PV owners to decide whether reactive power provision makes economic sense for their system configuration.

C. Economic Balance of Local Reactive Power Provision

Figure 10 presents the costs and benefits of reactive power provision from PV at different penetration levels. We can observe that in general, by increasing the PV penetration in a system, the benefits of reactive power injection (in [SGD/kvarh]) decreases, in line with what has been found in [12]. The spikes in the monetary benefits occur when PV is added at strategic locations (18.9%, 31.4%, 94.3%), as previously explained in Section VI-A.

⁴The simulation over at least a year is required to take into account the variation of inverter usage due to different weather conditions throughout the year.

However, as the PV penetration increases, the reactive power cost decreases, thanks to lower LR of the inverter. As a result, the net benefits from Q increases from 56.6% penetration onwards. The gap between the benefits from Q (the blue curve in Fig. 10) and the reactive power cost (the sum of the two areas in Fig. 10) is the possible range of monetary incentives that can be given to PV owners to inject reactive power.

According to the information in Figs. 8 and 10, it is evident that it is more efficient for the PV to inject smaller amount of reactive power, to reduce the losses in the system, but not to reduce the lifetime of the inverter significantly.

It is also noteworthy that the reduction in the inverter lifetime due to reactive power compensation can be a significant part of the reactive power cost, especially at lower penetration level ($c_t^{QPV, LR} > c_t^{QPV, invloss}$ until 31.4% PV penetration). In [12], [36], it has been found that reactive power provision from PV is competitive with switched capacitors. However, this may no longer be the case after considering the inverter LR.

VII. CONCLUSION

In this work, reactive power cost from photovoltaic systems (PVs) considering inverter lifetime reduction has been formulated and quantified. One-year simulations with real weather and load data for the case of Singapore at different PV penetration levels have been conducted to analyse the benefits of local reactive power provision to the system, and its effect on the lifetime of the PV inverters. The lifetime reduction cost has been shown to be a significant part of the reactive power cost and should be incorporated into optimization of reactive power dispatch. Accordingly, a simple polynomial relation between the inverter lifetime reduction cost and the PV reactive power output, which can be incorporated into any cost function, has been formulated.

Moreover, having a more distributed reactive power support from multiple PVs in the system has been shown to be beneficial, as the reactive power cost will be reduced, due to a lower reduction in the inverter lifetime. Therefore, the system operator can have a larger range for monetary compensation for the local reactive power provision.

The results from this work can be used as a foundation for future research on market mechanism or formulating strategies for reactive power provision from PV. Future work will also strive to establish relationships between reactive power provision and inverter lifetime for other types of inverters, capacitors, and systems.

REFERENCES

- [1] K. Bhattacharya and J. Zhong, "Reactive power as an ancillary service," *IEEE Trans. Power Syst.*, vol. 16, no. 2, pp. 294–300, May 2001.
- [2] R. G. Wandhare and V. Agarwal, "Reactive power capacity enhancement of a PV-grid system to increase PV penetration level in smart grid scenario," *IEEE Trans. Smart Grid*, vol. 5, no. 4, pp. 1845–1854, Jul. 2014.
- [3] L. Zhang, W. Tang, J. Liang, P. Cong, and Y. Cai, "Coordinated day-ahead reactive power dispatch in distribution network based on real power forecast errors," *IEEE Trans. Power Syst.*, vol. 31, no. 3, pp. 2472–2480, May 2016.

- [4] V. Kekatos, G. Wang, A. J. Conejo, and G. B. Giannakis, "Stochastic reactive power management in microgrids with renewables," *IEEE Trans. Power Syst.*, vol. 30, no. 6, pp. 3386–3395, Nov. 2014.
- [5] X. Su, M. A. Masoum, and P. J. Wolfs, "Optimal PV inverter reactive power control and real power curtailment to improve performance of unbalanced four-wire LV distribution networks," *IEEE Trans. Sustain. Energy*, vol. 5, no. 3, pp. 967–977, Jul. 2014.
- [6] H. T. Yang and J. T. Liao, "MF-APSO-based multiobjective optimization for PV system reactive power regulation," *IEEE Trans. Sustain. Energy*, vol. 6, no. 4, pp. 1346–1355, Oct. 2015.
- [7] T. Ding, C. Li, Y. Yang, J. Jiang, Z. Bie, and F. Blaabjerg, "A two-stage robust optimization for centralized-optimal dispatch of photovoltaic inverters in active distribution networks," *IEEE Trans. Sustain. Energy*, vol. 8, no. 2, pp. 744–754, Apr. 2017.
- [8] T. Sousa, H. Morais, Z. Vale, and R. Castro, "A multi-objective optimization of the active and reactive resource scheduling at a distribution level in a smart grid context," *Energy*, vol. 85, pp. 236–250, 2015.
- [9] O. Gandhi, W. Zhang, C. D. Rodríguez-Gallegos, D. Srinivasan, and T. Reindl, "Continuous optimization of reactive power from PV and EV in distribution system," in *Proc. IEEE Innovative Smart Grid Technol.*, Melbourne, VIC, Australia, Nov. 2016, pp. 281–287.
- [10] O. Gandhi, C. D. Rodríguez-Gallegos, and D. Srinivasan, "Review of optimization of power dispatch in renewable energy system," in *Proc. IEEE Innovative Smart Grid Technol.*, Melbourne, VIC, Australia, Nov. 2016, pp. 250–257.
- [11] M. Braun, "Provision of ancillary services by distributed generators," Ph.D. Thesis, Faculty of Elect. Eng./Comput. Sci., Kassel University, Kassel, Germany, 2008.
- [12] O. Gandhi, C. D. Rodríguez-Gallegos, W. Zhang, D. Srinivasan, and T. Reindl, "Economic and technical analysis of reactive power provision from distributed energy resources in microgrids," *Appl. Energy*, vol. 210, pp. 827–841, Jan. 2018.
- [13] A. Anurag, Y. Yang, and F. Blaabjerg, "Thermal performance and reliability analysis of single-phase PV inverters with reactive power injection outside feed-in operating hours," *IEEE J. Emer. Sel. Topics Power Electron.*, vol. 3, no. 4, pp. 870–880, Dec. 2015.
- [14] S. M. Sreechithra, P. Jirutitijaroen, and A. K. Rathore, "Impacts of reactive power injections on thermal performances of PV inverters," in *Proc. Ind. Electron. Conf.*, 2013, pp. 7175–7180.
- [15] H. Wang, Y. Yang, and F. Blaabjerg, "Reliability-oriented design and analysis of input capacitors in single-phase transformer-less photovoltaic inverters," in *Conf. Proc. IEEE Appl. Power Electron. Conf. Expo.*, 2013, pp. 2929–2933.
- [16] H. Wang *et al.*, "Transitioning to physics-of-failure as a reliability driver in power electronics," *IEEE J. Emer. Sel. Topics Power Electron.*, vol. 2, no. 1, pp. 97–114, Mar. 2014.
- [17] H. Wang and F. Blaabjerg, "Reliability of capacitors for DC-link applications in power electronic converters—An overview," *IEEE Trans. Ind. Appl.*, vol. 50, no. 5, pp. 3569–3578, Sep./Oct. 2014.
- [18] A. Albertsen, "Electrolytic capacitor lifetime estimation," 2010. [Online]. Available: <http://www.powerguru.org/electrolytic-capacitor-lifetime-estimation/>
- [19] T. Stetz, M. Rekinger, and I. Theologitis, "Transition from uni-directional to bi-directional distribution grids," Int. Energy Agency, Kassel, Germany, Tech. Rep. IEA PVPS T14-03:2014, 2014.
- [20] K. Ding, X. Bian, H. Liu, and T. Peng, "A MATLAB-simulink-based PV module model and its application under conditions of nonuniform irradiance," *IEEE Trans. Energy Convers.*, vol. 27, no. 4, pp. 864–872, Dec. 2012.
- [21] C. D. Rodríguez-Gallegos *et al.*, "A siting and sizing optimization approach for PV Battery Diesel hybrid systems," *IEEE Trans. Ind. Appl.*, vol. 54, no. 3, pp. 2637–2645, May 2018.
- [22] J. D. Flicker, R. Kaplar, M. Marinella, and J. Granata, "PV inverter performance and reliability: What is the role of the bus capacitor?" in *Proc. 38th IEEE Photovoltaic Specialists Conf.* Austin, TX, USA, Jun. 2012, pp. 1–3.
- [23] D. Ton and W. Bower, "Summary report on the DOE high-tech inverter workshop," U.S. Dept. Energy, Washington, DC, USA, 2005. [Online]. Available: https://www1.eere.energy.gov/solar/pdfs/inverter_II_workshop.pdf
- [24] D. G. Holmes and T. A. Lipo, *Pulse Width Modulation for Power Converters*. Piscataway, NJ, USA: IEEE Press, 2003.
- [25] J. Kolar and S. Round, "Analytical calculation of the RMS current stress on the DC-link capacitor of voltage-PWM converter systems," *IEE Proc. Elect. Power Appl.*, vol. 153, no. 4, pp. 535–543, Jul. 2006.
- [26] M. Bieri, K. Winter, S. Tay, A. Chua, and T. Reindl, "An irradiance-neutral view on the competitiveness of life-cycle cost of PV rooftop systems across cities," *Energy Procedia*, vol. 130, pp. 122–129, 2017.
- [27] C. D. Rodríguez-Gallegos, D. Yang, O. Gandhi, M. Bieri, T. Reindl, and S. K. Panda, "A multi-objective and robust optimization approach for sizing and placement of PV & batteries in off-grid systems fully operated by diesel generators: An Indonesian case study," *Energy*, to be published.
- [28] O. Gandhi, W. Zhang, C. D. Rodríguez-Gallegos, M. Bieri, T. Reindl, and D. Srinivasan, "Analytical approach to reactive power dispatch and energy arbitrage in distribution systems with DERs," *IEEE Trans. Power Syst.*, to be published.
- [29] M. E. Baran and F. F. Wu, "Network reconfiguration in distribution systems for loss reduction and load balancing," *IEEE Trans. Power Del.*, vol. 4, no. 2, pp. 1401–1407, Apr. 1989.
- [30] Trina Solar, "Allmax M Plus Framed 60-cell Module," 2017. [Online]. Available: http://static.trinasolar.com/sites/default/files/Datasheet_Allmax_M_Plus_DD05.xx%28II%29_US_July2017_C_0.pdf
- [31] Vishay, "Aluminum capacitors, power general purpose screw terminals," 2017. [Online]. Available: <https://www.vishay.com/docs/28390/500pgpst.pdf>
- [32] T. Messo, J. Jokipii, J. Puukko, and T. Suntio, "Determining the value of DC-link capacitance to ensure stable operation of a three-phase photovoltaic inverter," *IEEE Trans. Power Electron.*, vol. 29, no. 2, pp. 665–673, Feb. 2014.
- [33] J. S. Savier and D. Das, "Impact of network reconfiguration on loss allocation of radial distribution systems," *IEEE Trans. Power Del.*, vol. 22, no. 4, pp. 2473–2480, Oct. 2007.
- [34] Energy Market Authority, "Singapore Half-hourly System Demand Data," 2017. [Online]. Available: https://www.ema.gov.sg/statistic.aspx?sta_sid=20140826Y84sgBebjwKV
- [35] EMC, "Energy Market Company Price Information," 2017. [Online]. Available: <https://www.emcsg.com/marketdata/priceinformation>
- [36] O. Gandhi, D. Srinivasan, C. D. Rodríguez-Gallegos, and T. Reindl, "Competitiveness of reactive power compensation using PV inverter in distribution system," in *Proc IEEE PES Innovative Smart Grid Technol. Conf. Eur.*, Torino, Italy, Sep. 2017, pp. 1–6.



Oktoviano Gandhi (S'16) received Master of Physics degree from the University of Oxford, Oxford, U.K., in 2015. He is currently working toward the Ph.D. degree at the Graduate School for Integrative Sciences and Engineering and the Solar Energy Research Institute of Singapore, National University of Singapore, Singapore. His research interests include integration of solar energy into power systems, especially in the fields of optimization and reactive power dispatch.



Carlos D. Rodríguez-Gallegos (S'16) received the B.Eng. degree (rank 1) in electrical engineering with specialization in electronics and industrial automation from the Escuela Superior Politécnica del Litoral, Guayaquil, Ecuador, in 2011, and the M.Sc. degree (rank 1) in energy science and technology from the University of Ulm, Ulm, Germany, and Fraunhofer ISE, Freiburg, Germany, in 2014. He is currently working toward the Ph.D. degree with the Department of Electrical and Computer Engineering, National University of Singapore, Singapore.

He is a Research Assistant with the Solar Energy Research Institute of Singapore, Singapore. His research interests include photovoltaics, optimization design, and power electronics.



Naga Brahmendra Yadav Gorla (S'15) received the M.S. degree from Indian Institute of Technology, Madras (IITM), Chennai, India, in 2013. He was with the Electrical Engineering Department, Singapore Polytechnic as a Research Engineer between October 2013 and December 2015. Since January 2015, he has been with the Electrical Machines and Drives Lab, National University of Singapore, Singapore, as a Ph.D. candidate. His research interests include power quality improvement in grid connected inverters and rectifiers, fault tolerance and resiliency in multilevel converters, solid state transformer architectures and control.



Thomas Reindl received the master's (Hons.) degree in chemistry, the Ph.D. (Hons.) degree in natural sciences, and the M.B.A. (Hons.) degree from the Institut Europen d' Administration des Affaires (INSEAD), Fontainebleau, France, in 1994, 1996, and 2001, respectively. He is the Deputy CEO of the Solar Energy Research Institute of Singapore (SERIS), Singapore, and the Principal Research Fellow with the National University of Singapore, Singapore. In 1992, he joined SIEMENS Corporate Reserach and Development Labs, where he worked on photovoltaics (PVs). After holding several management positions at SIEMENS and running one of the leading German PV systems integration companies as the Chief Operating Officer, he joined SERIS in 2010 and soon became the Director of the Solar Energy System cluster. His research interests include high-performance PV and embedded systems, technoeconomic road mapping, and the reliable integration of renewable energies into power systems. During his time at SERIS, he was a recipient of public research grants in excess of SGD 20 million, founded two spin-off companies, and authored strategic scientific papers such as the "PV Roadmap for Singapore."



Monika Bieri received the bachelor's degree of economics in 1999 from the University of Applied Science in business administration, Zurich, Switzerland, finished the Chartered Financial Analystist (CFA) in 2003 and completed the executive programme "Diploma of Advanced Studies in Renewable Energy Management (REM-HSG)" at the University of St. Gallen, St. Gallen, Switzerland, in 2013. She started her career in banking where she was responsible for analysing and forming investment recommendations of the utility sector in Europe for UBS. In 2014, she was with the Solar Energy Research Institute of Singapore where she performed various economic viability assessments of solar applications. Her research interests include life-cycle cost, grid parity analysis, and cashflow sensitivity analysis, as well as probability-based impact risk assessment and future power price scenario modeling.



Dipti Srinivasan (M'89–SM'02) received the M.Eng. and Ph.D. degrees in electrical engineering from the National University of Singapore in 1991 and 1994, respectively. She was a Postdoctoral Researcher with the University of California, Berkeley, Berkeley, CA, USA, from 1994 to 1995, before joining the National University of Singapore, where she is currently a Professor with the Department of Electrical and Computer Engineering. Her research interest is in the application of soft computing techniques to engineering optimization and control problems.